

SINTERED STEELS COATED WITH A CHROMIUM LAYER DOPED WITH DIAMOND NANOPARTICLES

Electrochemical Cr coatings doped with diamond nanoparticles were deposited on sintered steels with different carbon contents (0.2-0.8 wt.-%). The mechanical properties of surfaces as hardness and wear resistance increase as compared to the steel substrate. Microcutting and microgridding mechanisms were observed after tribological tests, but also adhesive wear in some areas was observed. X-ray examination indicated that the layer was textured, with the exception of the sample with the highest concentration of diamond nanoparticles in the electrolyte (42 g/l). The intensity ratio I_{Cr110}/I_{Cr200} was calculated and compared with the indices for a standard sample. The greatest differences in the intensity ratio occurred for the samples with low carbon content (0.2%C). On the other hand, more the material is textured the greater the difference.

Keywords: sintered steels, mechanical properties, coating layer

1. Introduction

Powder metallurgy is a high precision method with capability of producing parts with near net shape and complex form with high dimensional tolerance. However, some problems may arise during use of sintered parts because of their porosity. Porous items exhibit decrease in mechanical properties [1]. To overcome these problems coatings are applied. The electrochemical chromium coatings have a wide practical application. They increase the hardness and the wear resistance of the base material. The modification of the chromium galvanic coatings with diamond nanoparticles (ND) additionally increases the mechanical properties of the surface and of the item as a whole. Published studies refer to the influence of chromium layer modified by diamond nanoparticles coatings on dense materials [2-5]. The literature essentially reports morphological changes of the surface and increased microhardness and wear resistance of so modified Cr coatings. The maximum microhardness increase is about 2.5. Data on increased dry friction wear resistance are quite diverse: 15%, 1.4-1.8 times and up to 10 times [1-3]. The main goal of this study was to investigate the influence of the ND on microhardness, wear resistance and other mechanical properties of electrolytic chromium coatings applied on sintered ferrous products.

2. Experimental materials and methods

Electrochemical Cr coatings doped with diamond nanoparticles (ND) produced by detonation synthesis [6], were de-

posited on a powder metallurgy steel based on commercial NC 100.24 iron powder with different C contents (0.2, 0.4, 0.6 and 0.8 wt.-%) added in the form of ultrafine graphite. Processing conditions were: single pressing at 660 MPa followed by sintering at 1250°C in 5%H₂-95%N₂ mixture for 60 minutes. After sintering, steel samples with geometry according to PN-EN ISO 2740, were electrolytically treated. The chromium was deposited on the surface of the sintered items by an electrolytic process with the traditional acidic electrolyte containing CrO₃ – 220 g/l and H₂SO₄ – 2.2 g/l. The parameters of the electrolytic process were: current density – 45 A/dm²; duration of the process – 45 minutes and temperature of the electrolyte – 50°C. The ND were added to the electrolyte as an aqueous suspension at concentrations (C_{ND}) of 10, 25 and 42 g/l. Uncoated and coated samples were physically (density), mechanically (tensile) and wear tested. As-sintered densities were calculated by the geometrical method. Tensile tests were done at room temperature. During tensile testing, on MTS 810 instrument, according to 10002-1 standard, the cross-head speed was 1 mm/min. The ultimate tensile strength (UTS) and 0.2% offset yield strength (R_{p0.2}) were determined from the engineering stress-strain diagram. Elongation was measured using geometric method. The wear tests were carried out using the block-on-ring tester Tribosystem T05. The wear test conditions are presented in Fig. 1.

After mechanical tests, diffraction examinations were carried out using D8 Advanced diffractometer with cobalt anode – $\lambda = 0,179$ nm monochromatic radiation; the geometry of constant angle (grazing incidence, $\alpha = 3^\circ$). X-ray investigations were conducted using 2θ angle ranging from 30° to 130°,

* INSTITUTE OF METAL SCIENCE, EQUIPMENT AND TECHNOLOGIES-BAS, 67 SHIPCHENSKI PROHOD BLVD, 1574 SOFIA, BULGARIA

** AGH UNIVERSITY OF SCIENCE AND TECHNOLOGY, FACULTY OF METALS ENGINEERING AND INDUSTRIAL COMPUTER SCIENCE, AL. MICKIEWICZA 30, 30-059 KRAKOW, POLAND

Corresponding author: sulek@agh.edu.pl

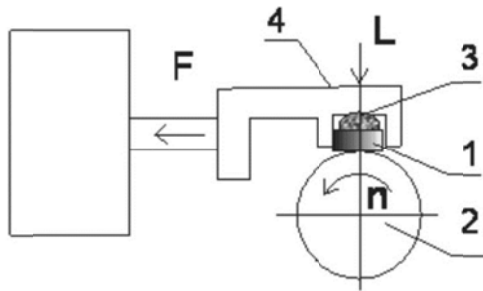


Fig. 1. Wear test principle of Tribosystem T05: 1 – wear sample, 2 – 100Cr6 steel ring, 3 – hemispherical insert, 4 – sample holder; conditions: test sample dimensions: $20 \times 4 \times 4$ mm, rotational speed: 136 r/min., load: 165 N, sliding distance: 500 m

where $\Delta 2\theta = 0.02^\circ$. Finally SEM analyses were carried out. Scanning electron microscopy (SEM) investigations were performed using Zeiss Merlin Gemini 2 microscope equipped with Bruker EDX microanalysis system. Specimens for SEM investigations were hot mounted in a conductive resin. After that specimens were ground and polished.

3. Results

Mechanical properties of uncoated and coated Fe-C sintered steels, together with their friction coefficients, are presented in Tables 1 and 2, respectively. The friction coefficient was calculated as mean force F [N] during the whole wear test divided by load (in Newtons).

Figures 2-5 present Fe-(0.2÷0.8)%C sintered and coated steel surfaces after wear testing.

The results of SEM investigation are summarised in Figs. 6-9, which show that the substrate (sintered steel) exhibits some porosity, whereas coating on the specimen was dense with a low number of defects (Fig. 6). Line profile of coated Fe-0.2%C steel (Fig. 7) showed Cr enrichment in the investigated coating. Similar observations were made on coatings (Fig. 8) with high Cr concentration (Fig. 9) on Fe-0.8%C specimens, where the porosity of the bulk material and the dense coating at the top are visible.

Tables 3 and 4 present the intensity ratios $I_{\text{Fe}\alpha 110}/I_{\text{Fe}\alpha 200}$ and $I_{\text{Cr}110}/I_{\text{Cr}200}$ comparing with the indices for a standard sample.

TABLE 1

The properties of uncoated steels – mean values (of 5 samples) and standard deviations

Steel composition	As-sintered density, g/cm ³	UTS, MPa	R _{p0.2} , MPa	A _{tot} , %	Matrix hardness, HV 0.25	Friction coefficient
Fe-0.2C	6.78±0.01	297±8	222±4	11.7±0.1	171-219	0.798±0.01
Fe-0.4C	6.77±0.01	340±22	246±11	7.8±0.2		0.763±0.02
Fe-0.6C	6.78±0.01	389±6	285±12	6.3±0.1		0.695±0.01
Fe-0.8C	6.74±0.01	467±18	345±10	6.9±0.1		0.651±0.02

TABLE 2

The properties of coated steels – mean values (of 5 samples) and standard deviations; C_{ND} = 25 g/l

Steel composition	As-sintered density, g/cm ³	UTS, MPa	R _{p0.2} , MPa	A _{tot} , %	Layer hardness, HV 0.25	Matrix hardness, HV 0.25	Friction coefficient
Fe-0.2C	6.78±0.01	331±9	242±13	8.9±0.1	774±62	171-219	0.517±0.01
Fe-0.4C	6.77±0.01	366±28	297±8	6.1±0.8	667±84		0.505±0.02
Fe-0.6C	6.78±0.01	405±3	376±16	5.0±0.1	648±86		0.582±0.01
Fe-0.8C	6.74±0.01	442±20	404±17	4.3±0.3	856±65		0.523±0.01

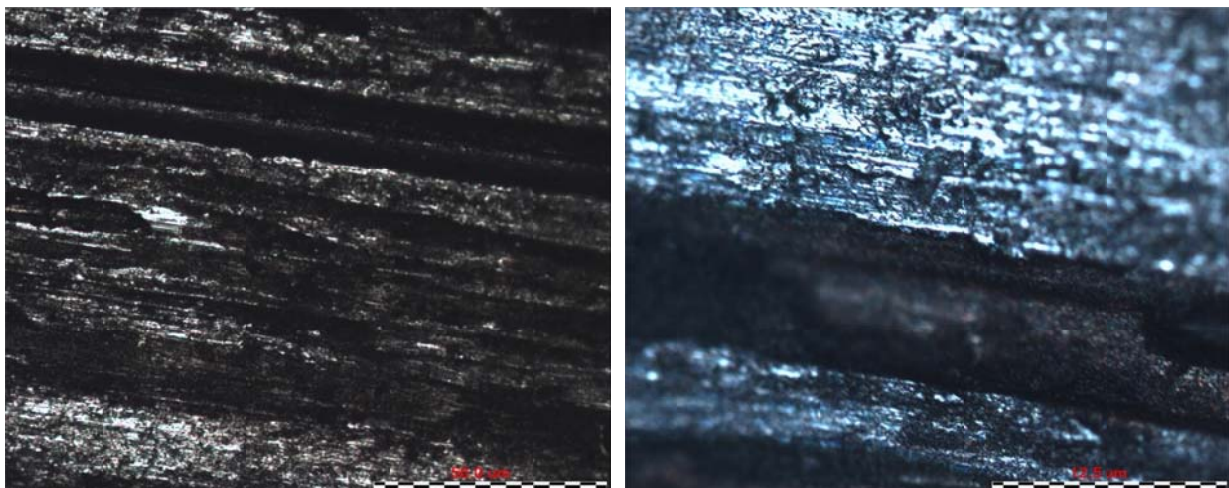


Fig. 2. The surface of the coated Fe-0.2%C sintered steel after tribological test; markers: 50 µm (left) and 12.5 µm (right)

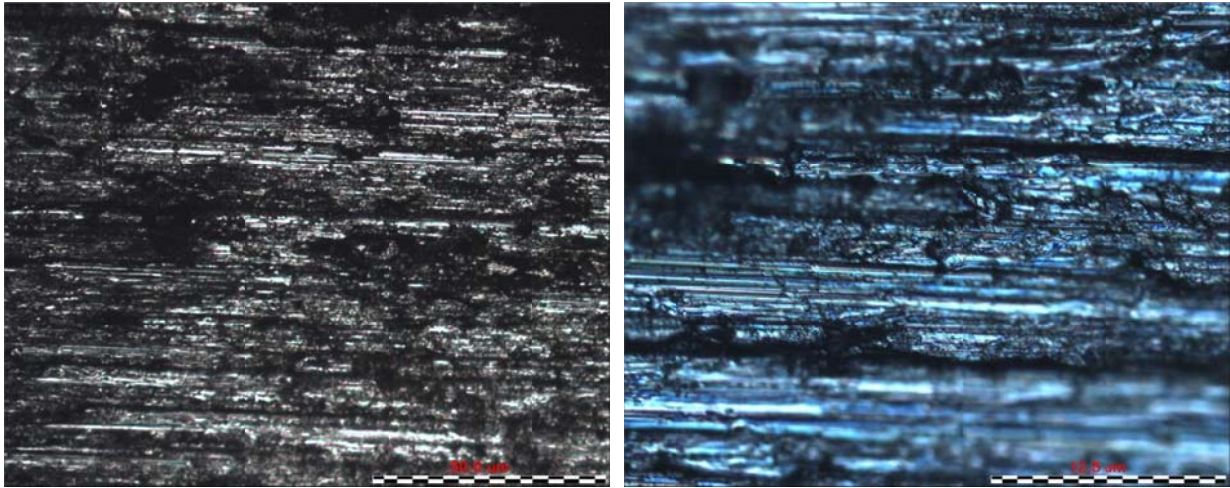


Fig. 3. The surface of the coated Fe-0.4%C sintered steel after tribological test; markers: 50 µm (left) and 12.5 µm (right)

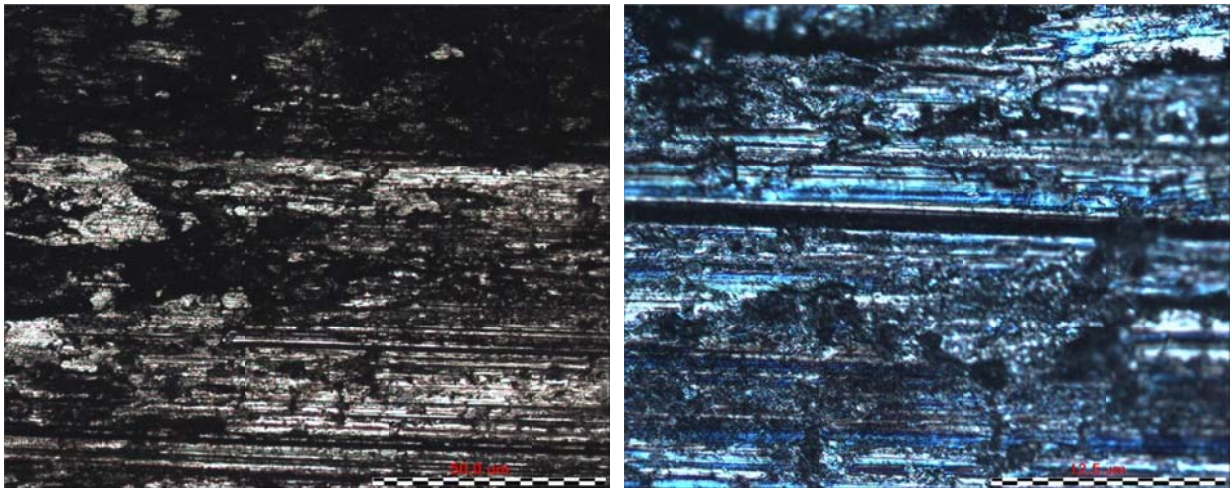


Fig. 4. The surface of the coated Fe-0.6%C sintered steel after tribological test; markers: 50 µm (left) and 12.5 µm (right)

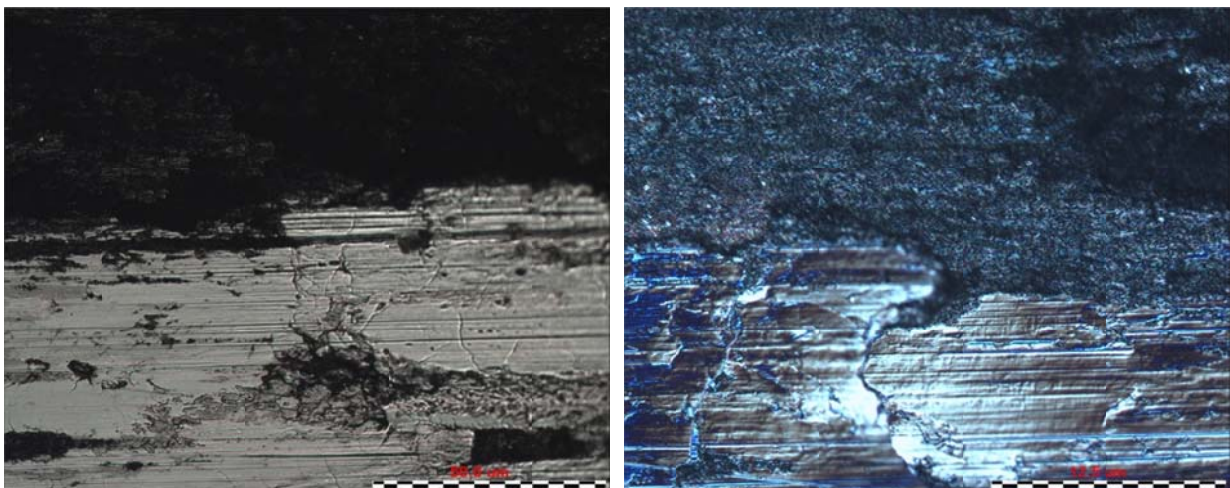


Fig. 5. The surface of the coated Fe-0.8%C sintered steel after tribological test; markers: 50 µm (left) and 12.5 µm (right)

Mentioned in table 4 intact and piece samples means samples, which were not mechanically tested and after mechanical tests, respectively. In Fig. 10, the XRD analyses of coated and uncoated steels are shown.

The diffraction patterns presented in Fig. 10a and 10b were obtained in geometry of constant angle $\alpha = 3^\circ$ with depth of X-ray penetration approx. 0.5 µm. The strongest peak is that chromium (110)_{Cr}. There was no peak from (200)_{Cr}. Peaks form

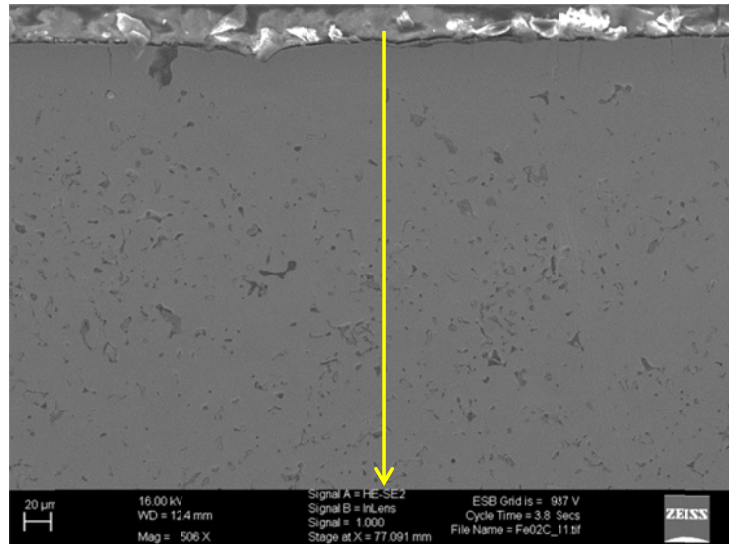


Fig. 6. Microstructure of coated Fe-0.2%C sintered steel; SEM

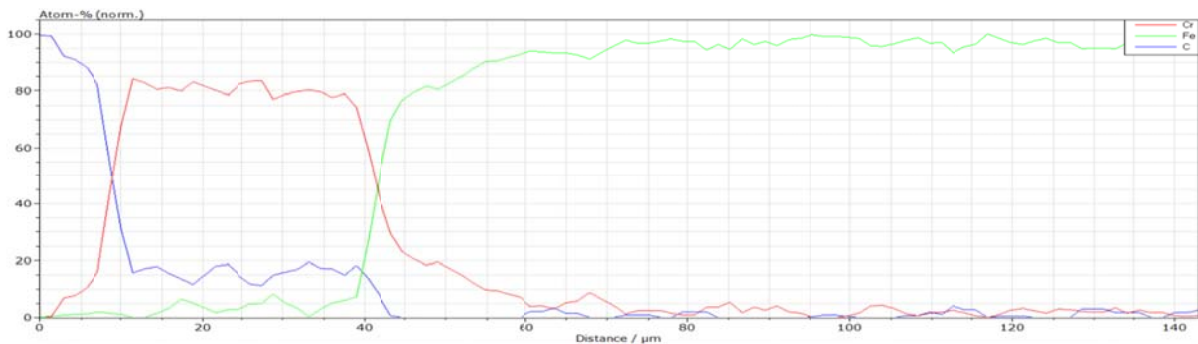


Fig. 7. Line profile of selected elements in coated Fe-0.2%C sintered steel

TABLE 3

The intensity ratio of uncoated steels

Sample No	Carbon content, %	I_{Fe110}/I_{Fe200}
Std. sample	—	5.0
5 ^{*)}	0.2	6.2
19 ^{*)}	0.4	8.8
40 ^{*)}	0.6	5.8
60 ^{*)}	0.8	7.4

Std. sample = powder sample without texture, ^{*)} uncoated samples

planes $(211)_{Cr}$ and $(220)_{Cr}$ were very weak. The diffraction patterns presented in Fig. 10b were similar to those presented in Fig. 10a – also the stronger peak came from plane $(110)_{Cr}$. For Fig. 10c the diffraction pattern were recorded in Bragg-Brentano geometry for uncoated Fe-(0.2-0.8%)C steels. In this case the depth of X-ray penetration was approx. 5 µm. On diffractograms the peaks came from planes of ferrite: (110), (200), (211), (220); the stronger peak was for plane (110).

Preliminary information data presented in Table 4 indicate that the layer was textured, except for the sample with the highest C_{ND} (sample no 14 – I_{Cr110}/I_{Cr200} ratio = 2.41 – Table 4). The greatest differences in the intensity ratio occurred for the samples with low carbon content (0.2%C). On the other hand, the higher these differences, the more the material is textured. The values

TABLE 4

The intensity ratio of coated steels
(current density = 45 A/dm²)

Sample No (kind of sample)	Carbon content, %	C_{ND} , g/l	I_{Cr110}/I_{Cr200}
Std. sample	—	—	2.50
4 (intact)	0.2	25	11.20
8 (intact)			22.30
11 (piece)			8.50
12 (piece)			18.80
13 (intact)	0.4	10	34.69
14 (piece)		42	2.41
24 (intact)	0.4	25	16.80
27 (intact)			15.60
28 (piece)			7.98
30 (intact)			12.20
34 (intact)	0.6	25	9.10
35 (intact)			8.50
44 (piece)			16.75
46 (intact)	0.8	25	19.98
50 (piece)			16.44
51 (intact)			14.54
58 (intact)	0.8	25	10.10

Std. sample = powder sample without texture, intact sample – sample which are not mechanically tested, piece sample – sample after mechanical test

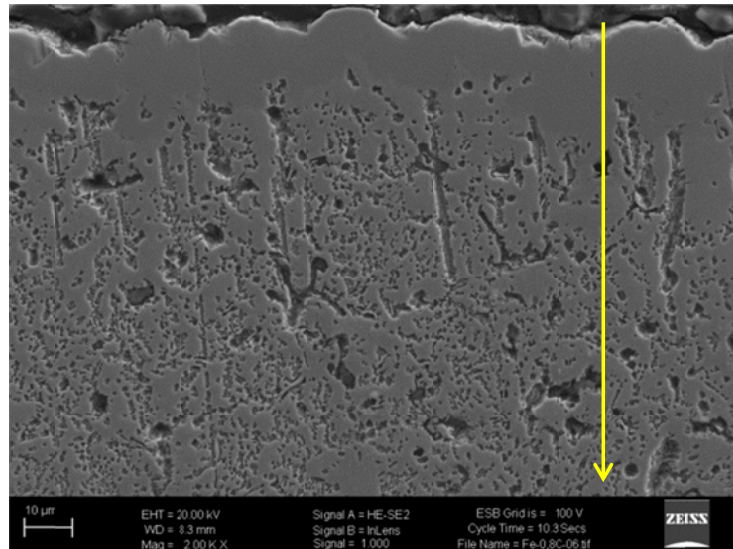


Fig. 8. Microstructure of coated Fe-0.8%C sintered steel; SEM

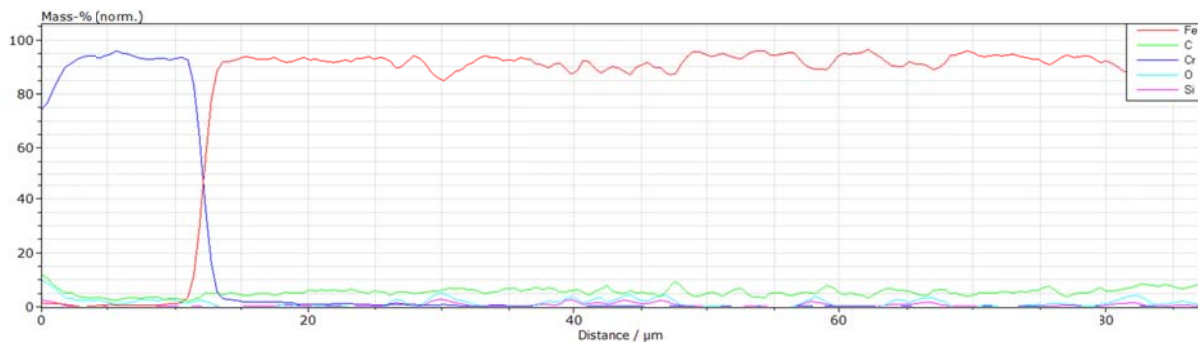


Fig. 9. Line profile of selected elements in coated Fe-0.8%C sintered steel

of intensity ratio for uncoated PM steels show small texture – maximal differences in the intensity ratio is 3.8.

4. Discussion

The data in Tables 1 and 2 show that increasing carbon concentration, of both uncoated and coated steels, increases mechanical properties, as reported in e.g. [7]. Regardless of chemical composition, strength properties (UTS, $R_{p0.2}$) are generally higher in the coated than those of the uncoated steels, but the presence of coating layer decreases plasticity. The reason of such phenomena is the presence of Cr in the layer and its high affinity for carbon. On the other hand, the mechanical properties coated steel samples are lower than those reported in e.g. [8-10].

As can be seen from Figs. 2-5, the post-friction surface morphology of sintered steels containing 0.2, 0.4, 0.6% C and 0.8%C is similar. The major wear mechanism was adhesive wear combined with ridging and scratching. Increasing carbon concentration up to 0.8% resulted in a different wear mechanism (Fig. 5). For Fe-0.8%C coated steel it could be observed that there is also additionally a locally visible movement of the plastic matrix, in the direction of the friction process. The com-

mon feature of surfaces after friction is also presence of oxides, which indicates that oxidation is also taking place during the test. The coating layer improves the wear resistance of steels (their friction coefficient was in the range 0.5-0.58 – Table 2) in contrast to the uncoated Fe-(0.2÷0.8)%C (the friction coefficient higher then 0.6 – Table 1).

After wear testing the surface morphology depends strictly on the characteristics of the layer at a given point of tribological contact. In the thick layer area, abrasion of the base material was not detected. Dominant was abrasive wear and possible sticking to the counter-sample material. However, in regions with a much smaller layer thickness and regions where cracks occur, the base material is exposed. Presence of deep scratches and furrows and plastic displacement of the base material, both in the friction direction and the filling of surface pores, was found there, as well as oxides. Quick removal of the layer adversely affects the tribological properties, increasing both the attrition depth and locally the friction coefficient.

As can be seen from Figs. 6-9, the coatings are very good adjacent to the steel, regardless of its chemical composition. On the other hand the chemical composition of steel substrate influence on the layer thickness (Fig. 7 and 9) and amount of Cr deposited in the layer. For Fe-0.2%C sintered steel, the layer thickness

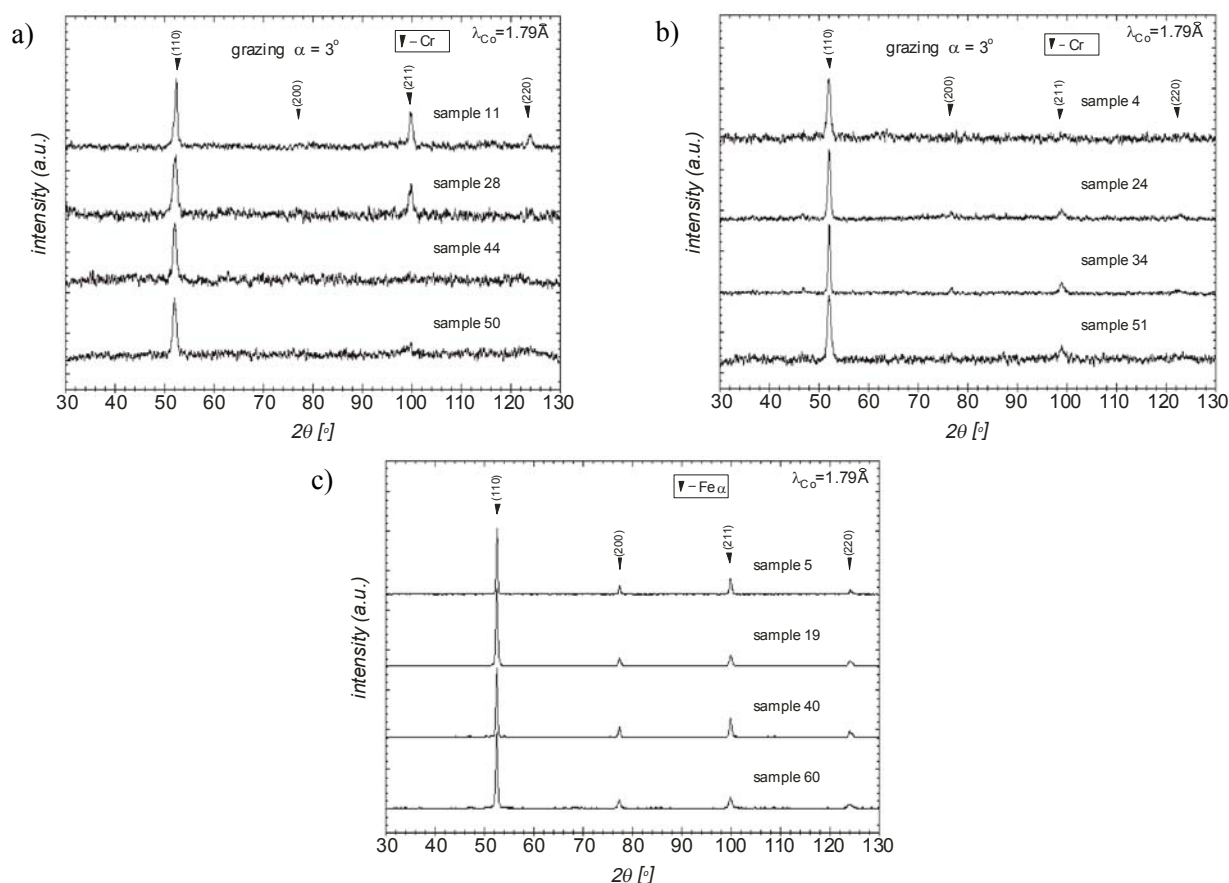


Fig. 10. XRD analysis of Fe-(0.2-0.8)%C steels; a) coated intact samples, b) pieces of coated samples c) uncoated samples (geometry Bragg-Brentano) – the numbers follow samples' description in Tables 3 and 4

was $\sim 30 \mu\text{m}$ and the amount of Cr was about 80% (Fig. 7), whereas for Fe-0.8%C this value was approximately three times lower ($\sim 10 \mu\text{m}$) and amount of Cr was closed to 90% (Fig. 9).

5. Summary

Electrochemical chromium coatings doped with diamond nanoparticles (ND) were deposited on sintered steels with different carbon contents (0.2-0.8 wt.-%). The mechanical properties of the surface increases as compared to the steel substrate. Microcutting and microgridding mechanisms were observed after the tribological tests, but also adhesive wear in some areas. The intensity ratio $I_{\text{Cr110}}/I_{\text{Cr200}}$ was calculated and compared with the indices for a standard sample. X-ray test provided us with some preliminary information that the layer was textured, with the exception of the sample with the highest C_{ND} (42 g/l). The greatest differences in the intensity ratio occurred for the samples with low carbon content (0.2%C). On the other hand, the greater these differences, the more the material is textured.

Acknowledgements

The work was conducted as a part of fundamental research financed by AGH University of Science and Technology project number 16.16.110.663. Part

of this study was performed with the financial support of the Fund "Scientific Researches" of the Bulgarian Ministry of Education and Science, Contract No DN 07/8/15.12.2016. The authors also would like to thank Prof. A.S. Wronski for editing this text.

REFERENCES

- [1] P. Leisner, R. Leu, P. Moller, Electroplating of Porous PM Compacts, *Powder Metall.* **40** (3), 207-210 (1997).
- [2] V. Dolmatov, T. Fujimura, G. Barkat, E. Orlova, M. Veretennikova, *Powder Metallurgy and Metal Ceramics* **42** (11-12), 587-591 (2003).
- [3] N. Mandich, J. Dennis, *Metal Finishing* **99** (6), 117-119 (2001).
- [4] V. Isakov, A. Lyamkin, D. Nikitin, A. Shalimova, A. Solntsev, *Protection of Metals and Physical Chemistry of Surfaces* **46** (5), 578-581 (2010).
- [5] N. Gidikova, A. Cias, V. Petkov, M. Madej, M. Sulowski, R. Valov, *Arch. Metall. Mater.* **59** (4), 1513-1516 (2014).
- [6] A. Krueger, *Journal of Materials Chemistry* **18**, 1485-1492 (2008).
- [7] K. Przybyłowicz, *Metaloznawstwo*, WNT, Warszawa (1992).
- [8] M. Sulowski, K. Faryj, *Arch. Metall. Mater.* **54** (1), 121-127 (2009).
- [9] M. Sulowski, *Powder Metallurgy*, **53** (2), 125-140 (2010).
- [10] M. Tenerowicz-Zaba, M. Sulowski, *Science of Sintering* **50** (4), 457-466 (2018).